Euclidean Farthest-Point Voronoi Diagram of a Digital Edge

Tristan Roussillon[b]

[a]*Université de Lyon, CNRS*
INSA-Lyon, LIRIS, UMR5205, F-69676, FRANCE

Euclidean Farthest-Point Voronoi Diagram of a Digital Edge

Tristan Roussillon[b]

[b]*Université de Lyon, CNRS*
INSA-Lyon, LIRIS, UMR5205, F-69676, FRANCE

Abstract

A digital edge is a digitization of a straight segment joining two points of integer coordinates. Such a digital set may be analytically defined by the rational slope of the straight segment. We show in this paper that the convex hull, the Euclidean farthest-point Voronoi diagram as well as the dual farthest-point Delaunay triangulation of a digital edge can be fully described by the continued fraction expansion of its slope.

Keywords: farthest-point Voronoi diagram, farthest-point Delaunay triangulation, convex hull, digital edge

1. Introduction

The Euclidean farthest-point Voronoi diagram of a set S of n point sites divides the plane into cells that consist of all the points that are farther from one site than from the $n-1$ others. Not every point site of S has a cell in the farthest-point Voronoi diagram. A point site has actually a cell iff it is a vertex of the convex hull of S[1][p. 164]. Let us recall that the convex hull of S is the intersection of all half-planes containing S. The farthest-point Delaunay triangulation of S is the planar dual to the Euclidean farthest-point Voronoi diagram of S. It is a triangulation of the convex hull of S such that the circumcircle of each triangle contains S.

In computational geometry, the closest-point and farthest-point Voronoi diagrams of an arbitrary set of point sites, as well as their dual triangulations, have been deeply studied (see *e.g.* [1, 2]). In digital geometry, the intersection of the closest-point Voronoi diagram with the fundamental lattice $\mathbb{Z}^2$ and the associated Euclidean distance transform have also been deeply studied (see [3] for a survey). This paper is a step towards the study of the Voronoi diagrams and Delaunay triangulations of analytical subsets of the fundamental lattice in order to understand their geometry.

In this paper, we focus on specific subsets of digital straight lines. The naive (resp. standard) line of slope a/b and intercept μ is the set of points $(x, y) \in \mathbb{Z}^2$ verifying $\mu \leq ax - by < \mu + \omega$ with a, b, μ, ω integers, $gcd(a, b) = 1$ and $\omega = \max(|a|, |b|)$ (resp. $\omega = |a| + |b|$). Note that the naive (resp. standard) line is simply 8-connected (resp. 4-connected) [4][p. 48, Proposition 3]. Points $(x, y) \in \mathbb{Z}^2$ such that $ax - by = \mu$ (resp. $ax - by = \mu + \omega - 1$) are called upper points (resp. lower points). The connected part of a digital straight line between two consecutive upper or lower leaning points is called a digital edge. The chain code of a digital edge is a Christoffel word. In shape analysis, digital edges are important because every digital curve that is locally convex has a unique decomposition into digital edges (see [5] or [6, 7] for a combinatorial point of view).

Without loss of generality, let us assume that the digital straight line lies in the first octant, *i.e.* $0 \leq a < b$, and that its intercept is null, *i.e.* $\mu = 0$. Both the origin $(0, 0)$ and the point (b, a) are upper points. They bound a naive (resp. standard) digital edge of slope a/b defined as

the set of points $(x, y) \in \mathbb{Z}^2$ verifying $0 \le ax - by < \omega$ and $0 \le x \le \omega$ (resp. $0 \le x + y \le \omega$).

We show in this paper that the farthest-point Delaunay triangulation of a standard digital edge is fully determined by the convergents of its slope. Equivalently, the farthest-point Voronoi diagram of a standard digital edge is fully determined by the convergents of its slope. However, we preferably work with the farthest-point Delaunay triangulation because its embedding involves only points of integer coordinates and even more, only extremal points of a digital edge. The farthest-point Delaunay triangulation of a standard digital edge of slope $12/29$ is illustrated in fig. 1.
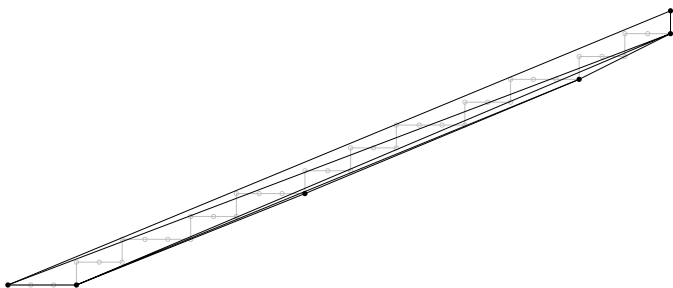

Figure 1: Farthest-point Delaunay triangulation of a standard digital edge of slope $12/29 = [0; 2, 2, 2, 2]$. Each convex hull vertex is depicted with a black dot. Other points are depicted with grey circles.

The motivation is two-fold. On one hand, we extend a previous work about the closest-point Voronoi diagram of a digital edge [8] with a study of the farthest-point Voronoi diagram of a digital edge. From these diagrams, we can determine for every point of the plane, its closest and farthest site, which may be useful to decide if two sets are circularly separable (see *e.g.* [9]). For instance, a standard digital edge and its copy translated by the vector $(1, 1)$ are depicted in fig. 2. Among the whole set of circles separating this digital edge from its translated copy, the extremal ones pass by three vertices of the closest and farthest-point Delaunay triangulation of the points. Hence, the present work is another step towards an analytical formula giving the smallest separating circle corresponding to a digital

straight segment. More generally, the present work will be useful to recognize digital circular arcs (or at least to efficiently initialize the recognition algorithm from a digital straight segment) and then estimate curvature, tangent and length.
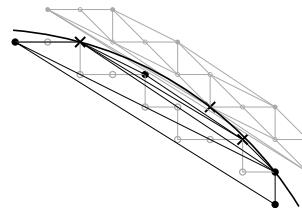

Figure 2: A digital edge and its copy translated by the vector $(1, 1)$. The smallest circle separating this digital edge from its translated copy is depicted in bold. It passes by two vertices of the farthest-point Delaunay triangulation of the enclosed digital edge and one vertex of the closest-point Delaunay triangulation of the translated copy.

On the other hand, determining the farthest-point Delaunay diagram of a digital edge is a toy problem to show how, for some incremental operations, an arithmetical and implicit representation can outperform a geometrical and explicit one. A simple example is the concatenation of two unimodular digital edges into a greater digital edge (see fig. 3). In [8], it is shown that the (closest-point) Delaunay triangulation of the resulting digital edge contains the Delaunay triangulation of the two base digital edges. For instance, we can see in fig. 3.a-b that the Delaunay triangulation of the digital edge of slope $5/8$ contains the Delaunay triangulation of the digital edges of slopes $3/5$ and $2/3$. Hence, when gluing together two unimodular digital edges, new triangular facets must be added to the data structure to maintain the triangulation, but nothing must be deleted (see fig. 3.b). Conversely, the same operation is catastrophic for the farthest-point Delaunay triangulation: the convex hull of the resulting digital edge must be triangulated from scratch (see fig. 3.c-d). However, we will see below that both the convex hull and the internal edges of the farthest-point Delaunay triangulation are fully described by the convergents of the slope of the digital edge
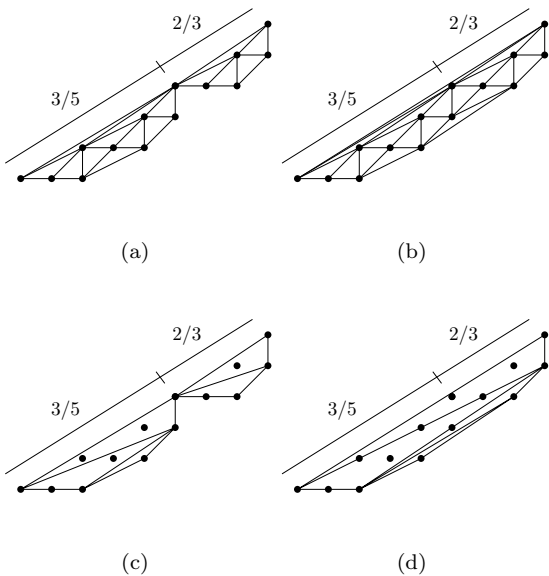
Figure 3: Update of the closest-point (a-b) and farthest-point (c-d) Delaunay triangulation after the concatenation of two unimodular digital edges.

and consequently, they can be implicitly maintained due to recurrence relations.

In this paper, we arithmetically characterize the farthest-point Delaunay triangulation of a standard digital edge. Since the farthest-point Delaunay triangulation of a point set is the farthest-point Delaunay triangulation of its convex hull [1][p. 164], we first arithmetically characterize the convex hull of a standard digital edge in section 2. Then, we show that this characterization also describes the structure of the farthest-point Delaunay triangulation in section 3. We end with some discussions about the extension of this result to a larger class of point sets.

2. Convex Hull of a Digital Edge

In this section, we introduce an arithmetical characterization of the convex hull of a digital edge. More precisely, we propose two recurrence relations that generate the vertices of the convex hull of a digital edge. In the next section, we will use the same relations to describe the structure of the farthest-point Delaunay triangulation of a digital edge.

2.1. Notations and digital edge definition

Let Σ be the set of lattice points belonging to the digital edge of direction vector $z(q, p)$ and of first point $O(0, 0)$, the origin. Let us assume without loss of generality that the components (q, p) of z, are such that $p, q \in \mathbb{Z}$, $1 \leq p < q$ and $\gcd(p, q) = 1$.

Note that vectors (resp. points) are denoted by lower case letters, *e.g.* z, (resp. upper case letters, *e.g.* $Z = O + z$).

Let $\wedge$ be the linear and antisymmetric operator $\mathbb{Z}^2 \times \mathbb{Z}^2 \mapsto \mathbb{Z}$ defined such that for all couple of vectors $v(x, y)$ and $v'(x', y')$, $v \wedge v' = xy' - yx'$. Note that the value $v \wedge v'$ is equal to the signed area of a parallelogram generated by v and v'.

Let s be a shift vector whose components are $(0, -1)$ in the naive case and $(1, -1)$ in the standard case. The introduction of vector s is a way of dealing with the naive and standard cases in the same unified framework, because $s \wedge z$ is the arithmetical thickness ω (equal to q in the naive case, but $p + q$ in the standard case) and $s \wedge v$ is the position of $v(x, y)$ (*i.e.* x in the naive case, but $x + y$ in the standard case). Our main result is valid only in the standard case (and that is why we illustrate only the standard case). However, we use this unified framework in order to point out which property is not valid in the naive case.

Due to the definition of a digital edge (given in section 1), Σ is defined as follows:

$$\Sigma = \left\{ O + v \in \mathbb{Z}^2 \ \middle| \ \begin{array}{c} 0 \leq v \wedge z < s \wedge z \\ \text{and } 0 \leq s \wedge v \leq s \wedge z \end{array} \right\}. \quad (1)$$

In order to avoid any sign ambiguity, s usually lies on the left hand side of the $\wedge$ operator, whereas z usually lies on its right hand side.

Let F (resp. G) be equal to $O - s$ (resp. $Z - s$). Geometrically, Σ is the set of lattice points located inside the parallelogram O, F, G, Z (where the side $[FG]$ is not included). The points are not randomly distributed, but their location is fully determined by z. We will see in the

4

next subsections that the geometry of the convex hull of a digital edge is fully determined by the components of the vector z.

The standard digital edge of direction vector $(8, 5)$ is depicted in fig. 4.
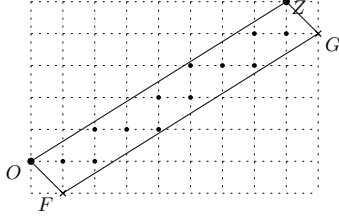

Figure 4: Standard digital edge lying between O and $Z(8, 5)$. The lattice points of the digital edge are depicted with black dots. They are located inside the parallelogram O, F, G, Z ($[FG]$ is not included).

2.2. Two recurrence relations

We now introduce the two following recurrence relations:

$$
\begin{aligned}
&u_0 = 0, \quad r_{-1} = s \wedge z, \, r_0 = p, \\
&\forall 1 \le k \le n, \, u_k = \left\lfloor \frac{r_{k-2}}{r_{k-1}} \right\rfloor, \, r_k = r_{k-2} - u_k r_{k-1}.
\end{aligned} \tag{2}
$$

$$
\begin{aligned}
&z_{-1} = -s, \, z_0 = (1, 0), \\
&\forall 1 \le k \le n, \, z_k = z_{k-2} + u_k z_{k-1}.
\end{aligned} \tag{3}
$$

The reader may recognize in (2) the sequence of quotients $\{u_k\}$ and the sequence of remainders $\{r_k\}$ returned by the Euclidean algorithm applied to p and q or p and $q + p$, depending on s. More precisely, in the naive (resp. standard) case, $p/q = [u_0; u_1, u_2, \ldots, u_n]$ (resp. $p/(p+q) = [u_0; u_1, u_2, \ldots, u_n]$).

In (3), the vectors of the sequence $\{z_k\}$ are called *convergents*, because they get closer to z as k gets closer to n (with $z_n = z$ as it will be shown in subsection 2.3). We will see in subsections 2.4 and 2.5 that the sequence $\{z_k\}$ characterizes the convex hull of digital edges of direction vector z. The convergents of $(8, 5)$, whose computation is detailed in tab. 1, are depicted in fig. 5.

k	−1	0	1	2	3	4
r	13	5	3	2	1	0
u		0	2	1	1	2
z	$(1, -1)$	$(1, 0)$	$(1, 1)$	$(2, 1)$	$(3, 2)$	$(8, 5)$

Table 1: Sequences of remainders, quotients and convergents computed from vector $(8, 5)$ (in the standard case with $s(1, -1)$).
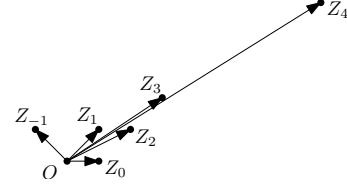

Figure 5: Graphical representation of the convergents of $z4(8, 5)$ (in the standard case with $s(1, -1)$).

2.3. Properties about remainders and convergents

There are close links between convergents. The following properties are known (see *e.g.* [10][Theorem 150, 151, 157]), but they are essential to prove the key lemmas 3 and 4 of section 3. They can be proved by induction by (2) and (3).

$$
\forall 0 \le k \le n \quad z_k \wedge z_{k-1} = q_k p_{k-1} - p_k q_{k-1} = (-1)^k. \tag{4}
$$

Note that (4) implies that $\forall -1 \le k \le n$, z_k is *irreducible*, *i.e.* its components are relatively prime. Indeed, z_{-1} is irreducible and for all $k \ge 0$, the greatest common divisor of the components of z_k, which divides $z_k \wedge z_{k-1} = (-1)^k$, is therefore equal to 1.

Using (3) and the linearity of $\wedge$, a straightforward corollary of (4) is:

$$
\forall 1 \le k \le n \quad z_k \wedge z_{k-2} = q_k p_{k-2} - p_k q_{k-2} = -u_k(-1)^k. \tag{5}
$$

Using (2) and (3), we can also prove by induction that the area of the parallelogram defined by z_k and z is equal to the remainder r_k:

$$
\forall -1 \le k \le n \quad z_k \wedge z = q_k p - p_k q = r_k(-1)^k. \tag{6}
$$

Moreover, we can similarly show that z is an aggregate of successive remainders and convergents:

$$
\forall 0 \le k \le n, \, r_k z_{k-1} + r_{k-1} z_k = z. \tag{7}
$$

5

By (2), remainders strictly decrease as k increases. Moreover,

$$r_n = 0 \quad \text{and} \quad r_{n-1} = \gcd(p, q) = 1. \tag{8}$$

The left part is trivial. In order to show the right one, it is enough to notice that

- on one hand, $\gcd(p, q)$, which divides both p and q, also divides $|z_k \wedge z| = r_k$ for all k ranging from -1 to n by (6), including r_{n-1}.

- on the other hand, r_{n-1} divides r_{n-2} and by induction, divides r_k for all k randing from -1 to $n-1$, and thus p and q.

To sum up:

$$r_{-1} = s \wedge z > p = r_0 > \ldots > r_{n-1} = 1 > r_n = 0. \tag{9}$$

Note that (7) and (8) clearly imply that $z_n = z$.

2.4. Convexity

Let us now introduce another sequence of points, $\{h_k\}$, defined from $\{z_k\}$, s and z as follows:

$$\forall -1 \le k \le n-1 \begin{cases} h_k = z_k + s & \text{if } k \text{ is odd,} \\ h_k = -z_k + z + s & \text{if } k \text{ is even.} \end{cases} \tag{10}$$

If k is odd, H_k is merely the translation of Z_k by vector s. If k is even, H_k is obtained by the composition of a point reflection across the origin O and a translation of vector $s + z$. Note moreover that $H_{-1} = O$.

The reader can compare Z_0, Z_1, Z_2, Z_3 in fig. 5 with H_0, H_1, H_2, H_3 in fig. 6.

Provided that $n > 1$ (resp. $n > 0$), let m_1 (resp. m_0) be the greatest odd (resp. even) positive integer strictly less than n, i.e. $m_1 = n-2$ (resp. $m_0 = n-1$) if n is odd and $m_1 = n-1$ (resp. $m_0 = n-2$) otherwise.

Let us focus now on the following circular list of points:

Definition 1. *(fig. 7) Λ is the circular list of points defined as follows: $O = H_{-1}$, H_1, ..., H_{2l+1}, ..., H_{m_1}, H_{m_0}, ..., H_{2l}, ..., H_0, Z (where the points H_k are defined from Z and s by (2), (3) and (10)).*
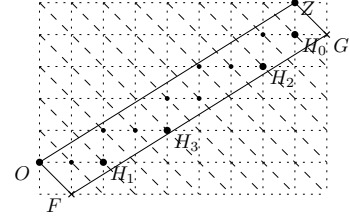

Figure 6: The points $O = H_{-1}$, H_1, H_3, H_2, H_0, Z_4, which are highlighted with bigger dots, have increasing positions, when measured by the intercepts of the diagonal dashed lines (see proposition 1).
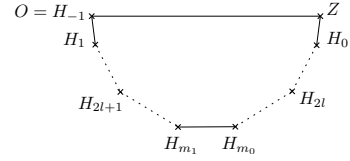

Figure 7: Graphical representation of Λ (definition 1). Points are depicted with crosses. Normal edges link consecutive points. Dotted edges indicate that an arbitrary number of extra points are lying between the two incident points (depending on the value of l and n).

Note that we have introduced above the integer l to easily distinguish an even index denoted by $2l$ from an odd index denoted by $2l + 1$.

In the next subsections, we prove that Λ is the list of vertices of the convex hull of the digital edge Σ in a counter-clockwise order. In this subsection, we first prove that Λ is a convex polygon.

Proposition 1. *(fig. 6) The points of Λ have increasing positions with respect to direction s, i.e. $0 < \ldots < s \wedge h_{2l+1} < \ldots < s \wedge h_{m_1} < s \wedge h_{m_0} < \ldots < s \wedge h_{2l} < \ldots < s \wedge z$.*

PROOF. The proof consists of three steps.

First, by (3), the positions of the convergents are in increasing order:

$$0 < s \wedge z_0 < s \wedge z_1 < \ldots < s \wedge z_{n-1} < s \wedge z_n. \tag{11}$$

Next, by (3), $s \wedge z_n = u_n(s \wedge z_{n-1}) + (s \wedge z_{n-2})$. Moreover, by (2) and (8), $r_{n-2} = r_n - u_n r_{n-1} = u_n$ and by (9), $u_n = r_{n-2} > 1$. As a consequence, we have:

$$s \wedge z_{n-1} < (s \wedge z_n)/2. \tag{12}$$

6

Finally, we separate convergents of odd and even index. For all $k = 2l + 1$ between 1 and m_1, it is clear that $s \wedge z_k = s \wedge h_k$. Hence, by (11) and (12), we obtain:

$$0 < s \wedge h_1 < \ldots < s \wedge h_{2l+1} < \ldots < (s \wedge z_n)/2.$$

Similarly, for all $k = 2l$ between 0 and m_0, $s \wedge h_k = s \wedge z_n - s \wedge z_k$. Hence, by (11) and (12), we obtain:

$$(s \wedge z_n)/2 < \ldots < s \wedge h_{2l} < \ldots < s \wedge h_1 < s \wedge z_n.$$

Putting all together, the vertices of Λ are actually ordered with respect to direction s as follows: $H_{-1} = O$ comes first, points of odd index in increasing order are followed by points of even index in decreasing order and $Z_n = Z$, i.e.

$$0 < \ldots < s \wedge h_{2l+1} < \ldots < s \wedge h_{m_1} < s \wedge h_{m_0},$$
$$s \wedge h_{m_1} < s \wedge h_{m_0} < \ldots < s \wedge h_{2l} < \ldots < s \wedge z.$$

$\square$

It is clear from proposition 1 that Λ is the list of vertices of a simple polygon in a counter-clockwise order. We additionally prove below that this polygon is convex.

Proposition 2. *(fig. 6) The orthogonal distance of the points of Λ to the straight line (OZ), multiplied by the length of the segment $[OZ]$, is a convex function,* i.e. $0 < \ldots < h_{2l+1} \wedge z < \ldots < h_{m_1} \wedge z$ *and* $h_{m_0} \wedge z > \ldots > h_{2l} \wedge z > \ldots > h_0 \wedge z$. *Moreover, its maximum is strictly less than* $s \wedge z$ *so that all the points of Λ belongs to the digital straight line of direction vector z and intercept* 0.

PROOF. By definition, O and Z belongs to the straight line (OZ) and have the minimal distance 0 to it. Consequently, let us focus on the other points.

For all k from 0 to $n - 1$, the orthogonal distance of H_k to the straight line (OZ) is equal to the area of the parallelogram defined by h_k and z, i.e. $|h_k \wedge z|$, divided by the length of the segment $[OZ]$, which is a constant that is independent of k.

By (10) and (6), $h_k \wedge z = -r_k + s \wedge z$ whatever the parity of k. Hence, by (6) and (9), it is clear that $0 < \ldots < h_{2l+1} \wedge z < \ldots < h_{m_1} \wedge z$ and $h_{m_0} \wedge z > \ldots > h_{2l} \wedge z > \ldots > h_0 \wedge z$.

Moreover, the maximum, is reached by $h_{n-1} \wedge z$ (with $n - 1 = m_1$ or $n - 1 = m_0$, depending on the parity of n) and is equal to $s \wedge z - r_{n-1} < s \wedge z$. As a consequence, all the points of Λ belongs to the digital straight line of direction vector z and intercept 0. $\square$

We have just proved that Λ is the list of vertices of a convex polygon in a counter-clockwise order.

Let Ω be the polygonal region whose boundary is defined as the list Λ in a counter-clockwise order. It is clear that Ω is the convex hull of the set Σ' of lattice points located inside Ω. Hence, in order to prove that Ω is the convex hull of Σ, it remains to show that $\Sigma' = \Sigma$ to conclude. This is done in the next subsection.

2.5. Lattice-based properties

To conclude, we need the two following lemmas:

Lemma 1. *There is no point of the fundamental lattice inside the parallelogram based on two consecutive convergents z_k and z_{k-1}, excepted its vertices.*

Lemma 1 is nearly a corollary of (4). See [10](forward implication of Theorem 32) and [10](Theorem 34 (i)) for further details.

This second lemma stems from lemma 1 and (5):

Lemma 2. *There is no point of the fundamental lattice inside the triangle O, Z_k, Z_{k-2}, excepted O and the u_k points lying exactly on the edge $[Z_k Z_{k-2}]$.*

We are now in position to prove the following Proposition:

Proposition 3. *All lattice points of Σ are located inside Ω.*

7

To prove proposition 3, it is enough to show that the complement of Ω in the parallelogram O, F, G, Z (which contains Σ by definition and Λ by proposition 1 and proposition 2), does not contain any lattice point in its interior.

As shown in fig. 8, the complement of Ω in the parallelogram O, F, G, Z can be partitioned into triangular facets that do not contain any lattice point in their interior by lemma 1 and lemma 2.
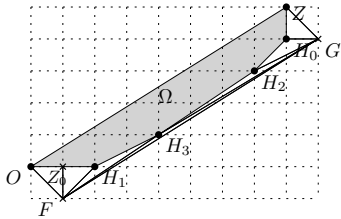

Figure 8: Triangulation of the complement of Ω (which is depicted in light grey) in the parallelogram O, F, G, Z. There are no lattice point in either triangles or on edges incident to a vertex of the parallelogram.

Together with proposition 1 and proposition 2, proposition 3 finally proves theorem 1.

Theorem 1. *Let Ω be the polygonal region whose boundary is defined as the list Λ in a counter-clockwise order (definition 1). Then, Ω is the convex hull of Σ.*

The connection between continued fractions and convex hull of a specific point set was observed by Klein in the nineteenth century as mentioned in [11]. This connection has been further used to design output-sensitive algorithms that retrieve the convex hull of analytical point sets such as the intersection of the fundamental lattice and a half-plane [12], a polygon [13], a disk [14]. Reveillès also observed a connection between continued fractions and the convex hull of the intersection of a lattice and an isothetic square [4, 15]. For the sake of completeness we have chosen to detail the connection between continued fractions and convex hull of digital edges, before showing a similar but totally new connection for the farthest-point Delaunay triangulation.

3. Farthest-Point Delaunay Triangulation of a Digital Edge

Let us introduce the following list of triangles:

Definition 2. *Let Γ be the list of triangles defined as follows: (H_0, O, Z), ..., (H_k, H_{k-1}, H_{k-2}), ..., $(H_{n-1}, H_{n-2}, H_{n-3})$ (where the points H_k are defined from Z and s by (2), (3) and (10)).*

Let (H_0, O, Z) be the 0-th triangle and (H_k, H_{k-1}, H_{k-2}) be the k-th triangle of Γ. Note that the k-th triangle of Γ is counter-clockwise oriented if k is odd and clockwise oriented otherwise.

If $n = 1$, Γ consists of the unique triangle (H_0, O, Z). In the rest of the section, we therefore assume that $n \geq 2$.

The goal of this section is to prove theorem 2.

Theorem 2. *In the standard case, i.e. if s is equal to $(1, -1)$, Γ is the farthest-point Delaunay triangulation of the digital edge Σ.*

3.1. Sketch of the proof

Proposition 4 and proposition 5 prove theorem 2.

Proposition 4. *Γ is a triangulation of the convex hull of Σ.*

Using the point order (proposition 1) and the convexity (theorem 2), proposition 4 is easily proved by induction (see fig. 9.a for the base case and fig. 9.b for the induction step).

Proposition 5. *In the standard case, i.e. if s is equal to $(1, -1)$, the circumcircle of each triangle in Γ contains Σ.*

Proving proposition 5 is more difficult. Our approach is to consider a pair of adjacent triangles in Γ. These two triangles share a common edge. They both have one opposite vertex, which is not incident to the common edge. The two following lemmas state that the circumcircle of the second triangle contains the opposite vertex of the first triangle.
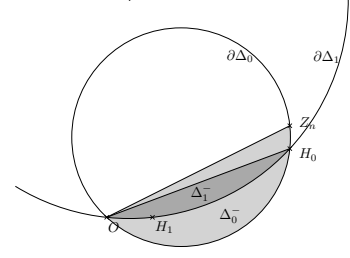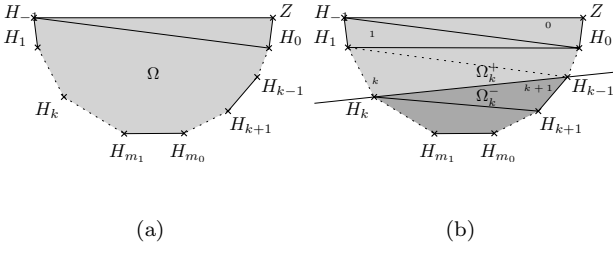
Figure 9: The first triangle of Γ trivially triangulate the part of Ω lying above the straight line $(H_{-1}H_0)$ (a). More generally, the first $(k+1)$ triangles of Γ triangulate Ω_k^+, the part of Ω lying above the straight line $(H_k H_{k-1})$. The $(k+1)$-th triangle lies in Ω_k^-, between $(H_k H_{k-1})$ and $(H_k H_{k+1})$ (b).

Lemma 3. *In the standard case,* i.e. *if s is equal to $(1,-1)$, the circle passing by O, H_1 and H_0 strictly contains $Z = Z_n$ for all $n \geq 2$.*

Lemma 4. *For all k such that $3 \leq k \leq n-1$, the circle passing by H_k, H_{k-1}, H_{k-2} strictly contains H_{k-3}.*

These two lemmas are key to prove proposition 5. They are proved in the next subsections using the relations between remainders and convergents highlighted in section 2.

Before giving the proof of proposition 5 by induction, we introduce the following notations. Let Δ_0 (resp. Δ_1) be the disk whose boundary is the circumcircle of H_0, O, Z_n (resp. H_1, H_0, H_{-1}). By convexity, the straight line passing through O and Z_n (resp. O and H_0) divides Δ_0 (resp. Δ_1) into two parts. For $k \in \{0,1\}$, let us denote the upper part (resp. lower part) by Δ_k^+ (resp. Δ_k^-).

By lemma 3, Δ_1 contains Z_n or, equivalently, Δ_0 contains H_1. By convexity, this implies that Δ_1^+ contains Δ_0^+ and that Δ_0^- contains Δ_1^-, *i.e.*

$$\Delta_0^+ \subset \Delta_1^+ \tag{13}$$

and

$$\Delta_1^- \subset \Delta_0^-. \tag{14}$$

Fig. 10 is an illustration of (14). The reader can similarly find out where are Δ_0^+ and Δ_1^+ in fig. 10 and check (13).

Figure 10: The boundary of the disks Δ_0 and Δ_1 are respectively depicted with a circle and a circular arc. The region colored in dark grey, denoted by Δ_1^-, is the part of the disk Δ_1 located below the straight line (O, H_0). It is included in the grey region (in light and dark grey), which is the part of the disk Δ_0 located below the straight line (O, Z_n) and denoted by Δ_0^-.

More generally, $\forall\, 2 \leq k < n$, let Δ_k be the disk whose boundary is the circumcircle of H_k, H_{k-1}, H_{k-2}. By convexity, the straight line passing through H_k and H_{k-1} divides Δ_k into two parts: the upper part denoted by Δ_k^+ and the lower one denoted by Δ_k^-. By lemma 4, $\forall\, 2 \leq k < n$, Δ_k contains H_{k-3}. As above, this implies that

$$\forall\, 2 \leq k < n, \quad \Delta_{k-1}^+ \subset \Delta_k^+ \tag{15}$$

and

$$\forall\, 2 \leq k < n, \quad \Delta_k^- \subset \Delta_{k-1}^-. \tag{16}$$

We are now in position to prove proposition 5 with two steps of strong induction. Note that the following proof is based on (13), (14), (15) and (16), which are derived from lemma 3 and lemma 4.

PROOF (OF PROPOSITION 5). Using (13) and (15), we prove by induction that $\forall\, 0 \leq k \leq n-1$, Δ_k^+ contains Z_n and all points H_l such that $-1 \leq l \leq k$.

Base cases: (0) By definition, Δ_0^+ contains O and Z_n. (1) By (13), Δ_1^+ contains Δ_0^+, which contains O and Z_n. Moreover, by definition, Δ_1^+ also contains H_0.

Induction step for $k > 1$: Let us assume that for some k such that $1 \leq k < n-1$, Δ_k^+ contains Z_n and all points H_l such that $-1 \leq l \leq k$. Let us prove that Δ_{k+1}^+ contains Z_n and all points H_l such that $0 \leq l \leq k+1$. By (15), Δ_{k+1}^+ contains Δ_k^+ and as a consequence, by the induction

9

hypothesis, Δ_{k+1} contains Z_n and all points H_l such that $-1 \leq l \leq k$. It remains the case of H_{k+1}, which is by definition on the boundary of Δ_{k+1}^+.

We can similarly show using (14) and (16) that $\forall 1 \leq k \leq n-1$, Δ_k^- contains all points H_l such that $k-2 \leq l \leq n-1$.

Moreover, Δ_0^-, which contains Δ_1^- by (14), contains Z_n and all points H_l such that $-1 \leq l \leq n-1$.

Putting all together, $\forall 0 \leq k \leq n-1$, Δ_k, which contains both Δ_k^+ and Δ_k^-, contains Z_n and all points H_l such that $-1 \leq l \leq n-1$. In other words, $\forall 0 \leq k \leq n-1$, Δ_k contains all the vertices of Ω, which concludes the proof. $\square$

Proposition 4 and proposition 5 straightforwardly prove theorem 2. It remains to prove lemma 3 and lemma 4. This is done in the next subsections.

3.2. Angle comparisons

The approach used to prove lemma 3 and lemma 4 can be coarsely described as follows. Let a convex quadrilateral be such that its four vertices V_0, V_1, V_2, V_3 are counterclockwise oriented. By basic geometry, it is clear that the circle passing by V_0, V_1, V_2 contains V_3 iff $(\overrightarrow{V_0V_1}, \overrightarrow{V_0V_2}) \geq (\overrightarrow{V_3V_1}, \overrightarrow{V_3V_2})$ (both oriented angles are positive by convexity).
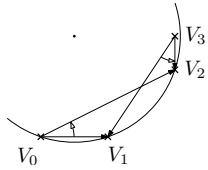

Figure 11: The circle passing by V_0, V_1, V_2 contains V_3 because the positive oriented angle $(\overrightarrow{V_0V_1}, \overrightarrow{V_0V_2})$ is greater than the positive oriented angle $(\overrightarrow{V_3V_1}, \overrightarrow{V_3V_2})$.

In order to compare two oriented angles, we compare their tangent because it can be computed by simple operations. Indeed, the tangent of the oriented angle between two given vectors $v(x,y)$ and $v'(x',y')$, is equal to the ratio between the sinus and the cosinus of the oriented angle,

which is equal to the ratio between $v \wedge v' = xy' - yx'$ and $v.v' = xx' + yy'$, i.e. $\tan(\overrightarrow{OV}, \overrightarrow{OV'}) = \frac{v \wedge v'}{v.v'}$.

3.3. Proof of lemma 3

PROOF. In order to show that the circle passing by O, H_1 and H_0 strictly contains $Z = Z_n$, we will show that

$$(\overrightarrow{OH_1}, \overrightarrow{OH_0}) > (\overrightarrow{Z_nH_1}, \overrightarrow{Z_nH_0}),$$

which is equivalent to showing that

$$\frac{h_0 \wedge h_1}{h_0.h_1} > \frac{(h_1 - z_n) \wedge (h_0 - z_n)}{(h_1 - z_n).(h_0 - z_n)},$$

provided that both numerators and denominators are positive.

The trick here is to notice that since $h_1 = (u_1, 0) = u_1(1, 0)$, we have:

$$\frac{h_0 \wedge h_1}{h_0.h_1} = \frac{h_0 \wedge (1, 0)}{h_0.(1, 0)}.$$

We can now independently compare numerators and denominators.

By (10), (2) and (3), we have in the standard case (with $s = (1, -1)$):

- $h_0 = -z_0 + z_n + s = (q_n, p_n - 1)$,

- $h_0 - z_n = -z_0 + s = (0, -1)$,

- $h_1 - z_n = z_1 + s - z_n = (u_1 - q_n, -p_n)$.

Denominators are:

$$h_0.(1, 0) = q_n \quad \text{and} \quad (h_1 - z_n).(h_0 - z_n) = p_n.$$

It is clear that $0 < (h_0 - z_n).(h_1 - z_n) < h_0.(1, 0)$, because we assume that $0 < p_n < q_n$.

Numerators are:

$$h_0 \wedge (1, 0) = p_n - 1 \quad \text{and} \quad (h_1 - z_n) \wedge (h_0 - z_n) = q_n - u_1.$$

Replacing q_n with $u_1 p_n + r_1$ by (2), we obtain $(h_1 - z_n) \wedge (h_0 - z_n) = u_1(p_n - 1) + r_1$. Though, $u_1(p_n - 1) \geq (p_n - 1)$ and $r_1 \geq 1$, because n is assumed to be greater than or equal to 2. Hence, $(h_1 - z_n) \wedge (h_0 - z_n) > h_0 \wedge (1, 0) > 0$.

Putting the two above results together, we obtain that both numerators and denominators are positive and that

$$\frac{h_0 \wedge h_1}{h_0 . h_1} > \frac{(h_1 - z_n) \wedge (h_0 - z_n)}{(h_1 - z_n).(h_0 - z_n)},$$

which concludes for the standard case. $\qquad \square$

Note that this result is the only one that is not valid in the naive case too. The reader may easily check that in the naive case (with $s = (0, -1)$), the circle passing by O, H_1 and H_0 does not contain Z, if $Z = (5, 3)$ for instance.

3.4. Proof of lemma 4

Contrary to lemma 3, lemma 4 does not depend on s and is valid both for the standard and naive cases.

PROOF. Let us recall that the k-th triangle of Γ is counter-clockwise oriented if k is odd and clockwise oriented otherwise.

In order to show that the circle passing by H_k, H_{k-1}, H_{k-2} strictly contains H_{k-3}, we show that

$$(\overrightarrow{H_{k-2}H_k}, \overrightarrow{H_{k-2}H_{k-1}}) > (\overrightarrow{H_{k-3}H_k}, \overrightarrow{H_{k-3}H_{k-1}})$$

if k is odd (angles are positive) and that

$$(\overrightarrow{H_{k-2}H_k}, \overrightarrow{H_{k-2}H_{k-1}}) < (\overrightarrow{H_{k-3}H_k}, \overrightarrow{H_{k-3}H_{k-1}})$$

if k is even (angles are negative).

Equivalently, let us compare

$$\alpha_k = \frac{(h_k - h_{k-2}) \wedge (h_{k-1} - h_{k-2})}{(h_k - h_{k-2}).(h_{k-1} - h_{k-2})}$$

with

$$\beta_k = \frac{(h_k - h_{k-3}) \wedge (h_{k-1} - h_{k-3})}{(h_k - h_{k-3}).(h_{k-1} - h_{k-3})}.$$

Using (2), (3) and (10), simple calculations lead to the following equalities, whatever the parity of k:

- $(h_{k-1} - h_{k-2}) = (z_n - z_{k-1} - z_{k-2})$,

- $(h_k - h_{k-2}) = (u_k z_{k-1})$,

- $(h_{k-1} - h_{k-3}) = (u_k z_{k-2})$,

- $(h_k - h_{k-3}) = (z_n - z_k - z_{k-3})$.

We can divide both numerators and denominators by u_k. Moreover, in order to make easier the comparisons, we transform these expressions using (3) and (7).

Solving (3) for z_{k-2} and multiplying the equality by -1, we obtain $-z_{k-2} = -z_k + u_k z_{k-1}$. Replacing $-z_{k-2}$ by $-z_k + u_k z_{k-1}$ and z_n with $r_k z_{k-1} + r_{k-1} z_k$ (7) in $(z_n - z_{k-1} - z_{k-2})$, we obtain the following equality:

$$(z_n - z_{k-1} - z_{k-2}) = (r_k - 1)z_{k-1} + (r_{k-1} - 1)z_k + u_k z_{k-1}.$$

Similarly, replacing $-z_{k-3}$ with $-z_{k-1} + u_{k-1} z_{k-2}$ (3) and z_n with $r_k z_{k-1} + r_{k-1} z_k$ (7) in $(z_n - z_k - z_{k-3})$, we obtain the following equality:

$$(z_n - z_k - z_{k-3}) = (r_k - 1)z_{k-1} + (r_{k-1} - 1)z_k + u_{k-1} z_{k-2}.$$

We are now in position to independently compare the numerators and denominators of

$$\alpha_k = \frac{z_{k-1} \wedge ((r_k - 1)z_{k-1} + (r_{k-1} - 1)z_k + u_k z_{k-1})}{z_{k-1}.((r_k - 1)z_{k-1} + (r_{k-1} - 1)z_k + u_k z_{k-1})}$$

and

$$\beta_k = \frac{((r_k - 1)z_{k-1} + (r_{k-1} - 1)z_k + u_{k-1} z_{k-2}) \wedge z_{k-2}}{(r_k - 1)z_{k-1} + (r_{k-1} - 1)z_k + u_{k-1} z_{k-2}).z_{k-2}}.$$

To shorten notations, let us denote by $N(.)$ (resp. $D(.)$) the numerator (resp. denominator) of any fraction. Developing the numerator $N(\alpha_k)$, we obtain $-(r_{k-1} - 1)(z_k \wedge z_{k-1})$. By (4), $(z_k \wedge z_{k-1})$ is equal to -1 if k is odd, but to 1 otherwise. Hence, $N(\alpha_k)$ is equal to $r_{k-1} - 1$ if k is odd, and to $-(r_{k-1} - 1)$ otherwise.

Developing the numerator $N(\beta_k)$, we obtain $(r_k - 1)(z_{k-1} \wedge z_{k-2}) + (r_{k-1} - 1)(z_k \wedge z_{k-2})$. By (4), $(z_{k-1} \wedge z_{k-2})$ is equal to 1 if k is odd and -1 if k is even. By (5), $(z_k \wedge z_{k-2})$ is equal to u_k if k is odd and $-u_k$ if k is even. Hence, $N(\beta_k)$ is equal to $(r_{k-1} - 1)u_k + (r_k - 1)$ if k is odd and to $-(r_{k-1} - 1)u_k - (r_k - 1)$ otherwise.

By (9), $r_{k-1} > r_k \geq 1$, because $k \leq n - 1$. We therefore conclude that $0 < N(\alpha_k) \leq N(\beta_k)$ if k is odd and that $N(\beta_k) \leq N(\alpha_k) < 0$ otherwise (with equality iff $r_k = 1$ and $u_k = 1$).

Developing the denominator $D(\alpha_k)$ we obtain

$$(r_k - 1)(z_{k-1}.z_{k-1}) + (r_{k-1} - 1)(z_k.z_{k-1}) + u_k(z_{k-1}.z_{k-1}),$$

and developing the denominator $D(\beta_k)$ we obtain

$$(r_k-1)(z_{k-1}.z_{k-2})+(r_{k-1}-1)(z_k.z_{k-2})+u_{k-1}(z_{k-2}.z_{k-2}).$$

Comparing denominators requires the two following results, which can be straightforwardly proved from (3).

On one hand, for all $v(x, y)$ such that $x \geq 0$ and $y \geq 0$:

$$\forall 1 \leq k \leq n \quad (z_k.v) > u_k(z_{k-1}.v) > (z_{k-1}.v) \geq 0. \quad (17)$$

On the other hand,

$$\forall 1 \leq k \leq n \quad (z_k.z_k) > u_k^2(z_{k-1}.z_{k-1}) \geq (z_{k-1}.z_{k-1}) \geq 1. \quad (18)$$

Finally, we conclude that $D(\alpha_k) > D(\beta_k) > 0$, because:

- $r_{k-1} > r_k \geq 1$ by (9).

- $(z_{k-1}.z_{k-1}) > (z_{k-1}.z_{k-2})$ by (17).

- $(z_k.z_{k-1}) > (z_k.z_{k-2})$ by (17).

- $u_k(z_{k-1}.z_{k-1}) \geq (z_{k-1}.z_{k-1}) > u_{k-1}(z_{k-2}.z_{k-2})$ by (18).

Putting results about numerators and denominators together, we conclude that

$$\frac{(h_k - h_{k-2}) \wedge (h_{k-1} - h_{k-2})}{(h_k - h_{k-2}).(h_{k-1} - h_{k-2})} > \frac{(h_k - h_{k-3}) \wedge (h_{k-1} - h_{k-3})}{(h_k - h_{k-3}).(h_{k-1} - h_{k-3})}$$

if k is odd and that

$$\frac{(h_k - h_{k-2}) \wedge (h_{k-1} - h_{k-2})}{(h_k - h_{k-2}).(h_{k-1} - h_{k-2})} < \frac{(h_k - h_{k-3}) \wedge (h_{k-1} - h_{k-3})}{(h_k - h_{k-3}).(h_{k-1} - h_{k-3})}$$

if k is even.

In both cases, this means that the circle passing by H_k, H_{k-1}, H_{k-2} strictly contains H_{k-3}. $\square$

4. Extension to Consecutive Digital Edges

We proved in section 3 that the farthest-point Delaunay triangulation of a *standard* digital edge is the list of triangular facets defined in definition 2 (see fig. 9 for a graphical representation). In other words, this triangulation is fully described by the convergents of the slope given

by (2) and (3). This result is valid for standard digital edges, but not for naive digital edge because of lemma 3.

This result is also true for consecutive standard digital edges. Let δ be an integer strictly greater than 1 and let us consider δ repetitions of a standard digital edge of direction vector z_n between the origin O and the point $Z = O + \delta z_n$.

With several minor modifications, we can show results similar to the ones of section 2 and section 3.

First, we slightly change the sequences of partial quotients, remainders and convergents, so that the n-th partial quotient equals 1 instead of being strictly greater than 1. The sequence of convergents

$$(z_{-1}, z_0, \ldots, z_{n-1}, z_n),$$

which is given by (2) and (3), becomes

$$(z_{-1}, z_0, \ldots, z_{n-1}, z_{n-2} + (u_n - 1)z_{n-1}, z_n)$$

This last sequence corresponds to the second possible representation of the continued fraction expansion of the pattern slope:

$$[u_0; u1, \ldots, u_{n-1}, u_n] = [u_0; u_1, \ldots, u_{n-1}, u_n - 1, 1].$$

Then, it is not difficult to prove propositions similar to proposition 1, proposition 2, proposition 3 and to show that the sequence of points $\{H_k\}$ (10) gives the vertices of the convex hull of δ repetitions of digital edges between O and Z.

In addition, neither proposition 4 nor proposition 5 change. Only lemma 3 and lemma 4 require to use $z = \delta z_n$ in place of z_n. This does not affect however the comparison of the numerators and denominators.

Consequently, the farthest-point Delaunay triangulation of δ repetitions of a standard digital edge of direction vector z is also fully determined by the sequence of convergents of z_n (see fig. 12).
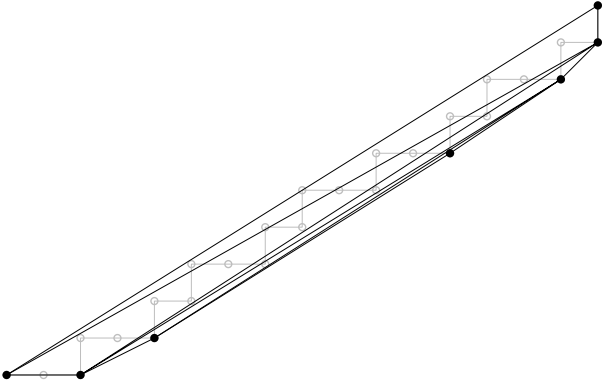
Figure 12: Farthest-point Delaunay triangulation of two consecutive standard digital edges of slope $5/8 = [0; 1, 1, 1, 1, 1]$ between O and Z ($z = 2z_5 = 2(8, 5) = (16, 10)$). Each convex hull vertex is depicted with a black dot. Other points are depicted with grey circles.

5. Conclusion

We showed in this paper that the farthest-point Delaunay triangulation (and equivalently the farthest-point Voronoi diagram) of a standard digital edge is fully described by the convergents of its slope. We showed that the triangulation topology is very specific. Let n be the index of the last convergent. The triangulation has exactly $n + 2$ vertices, $2n + 1$ edges ($n + 2$ on the boundary of the convex hull and $n - 1$ internal edges) and n facets (the Euler characteristic is equal to 1). Moreover, each facet share a common internal edge so that the facets can be ordered in a list (see definition 2 and fig. 9).

Repetitions of standard digital edges or standard digital straight segments of well-chosen length have the same topology. However, we do not observe the same topology for naive digital edges or arbitrary standard straight segments and our main perspective is to understand the geometry of the farthest-point Delaunay triangulation of such classes of point sets.

Eventually, note that the extended Euclidean algorithm provides a way to compute the farthest-point Delaunay triangulation of a pattern described by its slope p/q in the worst case in logarithmic time because $n = O(\log(q))$. In addition, when concatenating two unimodular digital edges (see section 1), the list of convergents can be updated in constant time and consequently the farthest-point Delaunay triangulation can be computed on demand in logarithmic time.

References

[1] M. de Berg, M. van Kreveld, M. Overmars, O. Schwarzkopf, Computational geometry: algorithms and applications, Springer-Verlag New York, Inc., Secaucus, NJ, USA, 1997.

[2] F. P. Preparata, M. I. Shamos, Computational geometry: an introduction, Springer-Verlag, New York, 1985.

[3] D. Coeurjolly, A. Vacavant, Separable distance transformation and its applications, in: V. E. Brimkov, R. P. Barneva (Eds.), Digital Geometry Algorithms, Vol. 2 of Lecture Notes in Computational Vision and Biomechanics, Springer Netherlands, 2012, pp. 189–214.

[4] J.-P. Reveillès, Géométrie discrète, calcul en nombres entiers et algorithmique, Ph.D. thesis, Université de Strasbourg (1991).

[5] T. Roussillon, I. Sivignon, Faithful polygonal representation of the convex and concave parts of a digital curve, Pattern Recognition 44 (10-11) (2011) 2693–2700.

[6] S. Brlek, J.-O. Lachaud, X. Provenal, C. Reutenauer, Lyndon christoffel digitally convex, Pattern Recognition 42 (10) (2009) 2239 – 2246.

[7] J.-O. Lachaud, X. Provenal, Two linear-time algorithms for computing the minimum length polygon of a digital contour, Discrete Applied Mathematics 159 (18) (2011) 2229 – 2250.

[8] T. Roussillon, J.-O. Lachaud, Delaunay properties of digital straight segments, in: Proceedings of the 16th IAPR international conference on Discrete geometry for computer imagery, Vol. 6607 of Lecture Notes in Computer Science, Springer-Verlag, Berlin, Heidelberg, 2011, pp. 308–319.

[9] S. Fisk, Separating point sets by circles, and the recognition of digital disks, IEEE Transactions on Pattern Analysis and Machine Intelligence 8 (4) (1986) 554–556.

[10] G. H. Hardy, E. M. Wright, An introduction to the theory of numbers (Fifth edition), Oxford Science Publications, Clarendon Press, London, 1979.

[11] H. Davenport, The Higher Arithmetic: Introduction to the Theory of Numbers, Oxford University Press, Oxford, 1983.

[12] H. Balza-Gomez, J.-M. Moreau, D. Michelucci, Convex hull of grid points below a line or a convex curve, in: Proceedings of the 8th international conference on Discrete geometry for computer imagery, Vol. 1568 of Lecture Notes in Computer Science, Springer Berlin Heidelberg, 1999, pp. 361–374.

[13] W. Harvey, Computing Two-Dimensional Integer Hulls, SIAM Journal on Computing 28 (6) (1999) 2285–2299.

[14] S. Har-Peled, An output sensitive algorithm for discrete convex hulls, Computational Geometry 10 (2) (1998) 125–138.

[15] J.-P. Reveillès, G. Yaacoub, A sublinear 3d convex hull algorithm for lattices, in: Proceedings of the 5th international conference on Discrete geometry for computer imagery, 1995, pp. 219–230.